

# Symbolic Relational Deep Reinforcement Learning based on Graph Neural Networks

Jaromír Janisch, Tomáš Pevný and Viliam Lisý

Artificial Intelligence Center, Department of Computer Science  
Faculty of Electrical Engineering, Czech Technical University in Prague  
{jaromir.janisch, tomas.pevny, viliam.lisy}@fel.cvut.cz

## Abstract

We present a novel deep reinforcement learning framework for solving relational problems. The method operates with a symbolic representation of objects, their relations and multi-parameter actions, where the objects are the parameters. Our framework, based on graph neural networks, is completely domain-independent and can be applied to any relational problem with existing symbolic-relational representation. We show how to represent relational states with arbitrary goals, multi-parameter actions and concurrent actions. We evaluate the method on a set of three domains: BlockWorld, Sokoban and SysAdmin. The method displays impressive generalization over different problem sizes (e.g., in BlockWorld, the method trained exclusively with 5 blocks still solves 78% of problems with 20 blocks) and readiness for curriculum learning.

## Introduction

In this work, we take a fresh look at the Relational Reinforcement Learning (RRL; Džeroski et al. 2001) with the modern approaches of Deep Reinforcement Learning (Deep RL). In contrast to the modern trend of applying Deep RL on the raw visual input (e.g., Mnih et al. 2015; Jaderberg et al. 2019), we target tasks of relational and symbolic nature. These are the tasks where the world consists of discrete *objects*, their *relations* and *actions* that manipulate these objects directly. Such tasks naturally occur all around us, the world itself is composed of objects on its macro-level. A simple task of cooking by a recipe integrates a complex system of objects in various relations and possible actions. Online services with API, social networks, computer network penetration testing, medical diagnosis, factory assembly line optimizations – these are all examples of environments, where these tasks are present.

Current Deep RL techniques are not prepared for these settings directly, as an usual requirement is that the state and action space dimensions are fixed. This is one of the reasons why the recent and Deep RL research focuses mostly on visual-control domains (e.g., Leibo et al. 2018). The described problems can certainly be transformed into visual control domains, however, this would bring an intermediary step into the process and is clearly suboptimal.

As an example, let’s look at a BlockWorld game (Slaney & Thiébaux 2001). Figure 1 shows how the game works: Initially, several labeled blocks are stacked on top of each

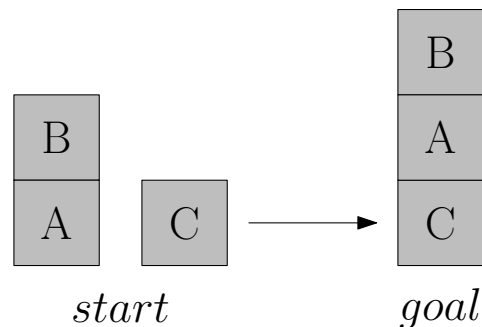


Figure 1: In the BlockWorld game, the task is to reconfigure the blocks into an arbitrary goal position. A single available action  $move(X, Y)$  relocates a block  $X$  on top of  $Y$  (if possible),  $Y$  can also be the *ground*. In this case, the optimal solution is a sequence of  $move(B, ground)$ ,  $move(A, C)$ ,  $move(B, A)$ . The key challenge is to generalize over arbitrary number of blocks with arbitrary labels.

other in an arbitrary configuration. The task is to reconfigure them into a goal position, using a *move* action, which picks a block a puts it on top of another, or to the ground.

In current Deep RL, there is no existing framework to solve the described task in a truly symbolic way. That is, using the *move* action with two symbolic parameters and *generalize well over arbitrary number of blocks*. The existing approaches usually solve a problem transformed into the pixel space, or with elementary non-parametrized actions (e.g., Li et al. 2019; Zambaldi et al. 2019).

In this work, we present a Symbolic Relational Deep RL (SR-DRL) framework. It accepts enriched symbolic input (i.e., abstract objects, optionally augmented with their features) and is designed to generalize well over arbitrary number of objects, their relations and multi-parameter actions.

The framework is primarily designed to find optimal solutions in domains which are a-priori symbolic relational. That is, an explicit enumeration of objects and relations is directly available. For other domains, recently resurfaced research direction of automatic object discovery (Garnelo et al. 2016; Zelinka et al. 2019) could be used.

Our framework’s main components are based on graph neural networks (Zhou et al. 2018) and auto-regressive policy

decomposition (Vinyals et al. 2017), joint with arbitrary policy gradient method (Li 2018). We showcase its capabilities in three domains. BlockWorld is a well-known planning domain with NP-hard complexity for optimal planning. We demonstrate impressive generalization of our method – the agent trained only on five blocks is able to solve environments with 20 block with 78% success rate. The two remaining domains are currently work-in-progress. Sokoban is a game requiring extensive planning. To demonstrate our framework, we replace native elementary actions with macro-actions, such as *push-left(block)*, while preserving all game rules. These actions are parametrized directly by the playing elements. Last domain, SysAdmin (Guestrin et al. 2001), is a probabilistic planning domain defined in International Probabilistic Planning Competition 2011.

### Contributions

1. We present a novel method that uses graph neural networks and reinforcement learning to solve relational problems. Our approach is completely domain-independent, with single requirement that the symbolic-relational representation of the problem already exists. We define the problem in the form of graphs and present a GNN based implementation<sup>1</sup>. We show how to represent relational states with arbitrary goals, multi-parameter actions and concurrent actions.
2. In a set of three domains (in this version, only BlockWorld is presented), we demonstrate the capabilities of our framework. For example, impressive generalization to different problem sizes or smooth curriculum learning.
3. As a minor contribution, we introduce an entropy regularization normalization, a technique for better scaling of reinforcement learning algorithms.

### Related work

Payani & Fekri (2020) replace the hard logic of Džeroski et al. (2001) with a differentiable inductive logic programming. In their approach, the logic predicates are fuzzy and the parameters are learned with gradient descent. BlockWorld environment is also used for experiments. However, the scope is very limited to only 4 and 5 blocks, without goal generalization (the goal is to always stack into a single tower) and the authors do not report any generalization capabilities.

Li et al. (2019) studies a 3-dimensional instantiation of the BlockWorld problem, with a robotic hand and physics simulation. Interestingly, the features of the blocks (their position and color) and the hand is encoded as a graph and processed by a graph neural network (GNN) (Zhou et al. 2018), making it invariant to the number of objects. Still, all interaction with the world is done through the control of the robotic hand and its elementary actions (relative change of position and grasping controls). Moreover, the blocks are not symbolic, but are identified by their features (color).

Hamrick et al. (2018) study the stability of a tower of blocks under a physical simulation, where some blocks can be *glued* together. The blocks are encoded as nodes in a graph, with only physical features, and the actions are performed on

the graph’s *edges*, which connect two adjoin blocks. Hence, the actions are performed onto the blocks themselves, making this approach generalize well to different combinations and numbers of blocks. However, this work is tied to this specific problem and does not provide a general framework. Comparatively, our work is completely domain-independent, can work with arbitrary, heterogeneous relations and multi-parameter actions.

Other works (Zambaldi et al. 2019; Santoro et al. 2017) provide specialized neural network architectures with relational inductive biases that try to internally segment a visual input into objects and process them relationally. Compared to our work, these architectures cannot process symbolic input.

In the domain of planning, Relational Dynamic Influence Diagram Language (RDDL) (Sanner 2010) can be used to describe a mechanics of an environment composed of objects, their relations and possible actions. Bajpai et al. (2018) describe an algorithm for training models that generalize over multiple problem instances in the same domain. Their model uses GNNs to encode the object relations, however the generalization is restricted to a fixed number of objects and actions. Also, a short retraining is required for the model to handle a new instance of the environment. Compared to this work, we do not impose any similar restrictions and, in the sense of transfer learning, our framework is completely zero-shot – there is no need for retraining with new instances.

Adjodah et al. (2018) studies a control problem of maze-navigation with a relational module. However, the studied problem is heavily restricted: it is a grid of a fixed size and the relations are represented as exhaustive binary combinations of all places in the grid. The output of the relational module is encoded as a fixed-size embedding and processed with a standard MLP based Q-learning algorithm. Also, no message passing is involved, allowing the model to reason only with the limited binary relations.

### Problem definition

Our problems naturally consists of *objects*, binary *relations*, *global context* and a *goal* definition. Moreover, our problems are sequential, hence we assume existing *transition* dynamics. We use the Markov Decision Process (MDP) formalism for following definitions. The MDP is a tuple  $(\mathcal{S}, \mathcal{A}, r, t, \gamma)$ , where  $\mathcal{S}$ ,  $\mathcal{A}$  represent the state and action spaces,  $r$ ,  $t$  are reward and transition functions and  $\gamma$  is the discount factor.

All of the MDP components are problem-dependent. The reward function  $r$  can directly specify the goal or be more subtle. For example, in the BlockWorld, the reward can be defined as a small negative value (e.g.,  $-0.1$ ) per step and a non-negative value when the goal is reached. The transition function  $t$  and parameter  $\gamma$  are directly defined by the particular environment. The definition of state and action spaces is more complex and is described below.

### State encoding

A state has to incorporate the key components – objects and their features, relations, global context and optionally the goal. The objects and relations naturally form an oriented graph, where the objects become nodes and the relations become edges.

<sup>1</sup>The code is at [github.com/jaromiru/sr-drl](https://github.com/jaromiru/sr-drl).

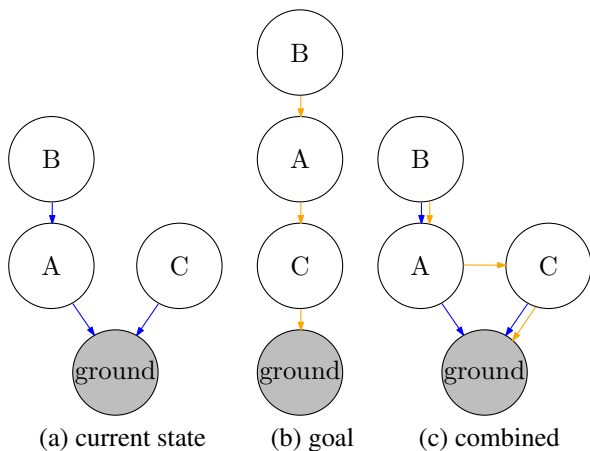


Figure 2: This example shows a graph representation of the BlockWorld game state from Figure 1. The objects are represented as nodes, their relations (*above-of*) as oriented edges. A special node represents the ground. Both the current state and the goal are encoded as a graph (with different edge types). The combined graph (the state encoding) contains all information needed to solve this problem. A single bit in each node differentiates the blocks from ground, no other features (e.g., labels) are present. Likewise, no global information is needed in this example.

The objects become the nodes of the graph and optionally contain their features in form of a fixed-length vector. More complicated structures can be embedded using the existing techniques (e.g., Pevný & Somol 2016; Zaheer et al. 2017). Heterogeneous objects can be recognized by a feature specifying their type.

The relations naturally form oriented edges of the graph. Symmetric relations can be transformed into two opposite edges. Similarly to objects, the relation’s type can be encoded as an edge’s feature.

Global context specify properties of the environment, unrelated to any single object (e.g., time, environment state, etc.). The features of the global context form a separate fixed-length vector, beside the object-relation graph.

In simple static-goal settings, only the reward function is sufficient to encode the goal definition. However, more often, the goal is part of a particular problem instance, and hence it has to be included in the state. Dependent on the problem, the goal can be encoded as part of the global context, in the object features, or as part of the graph itself.

The particular definition of the state space  $\mathcal{S}$  is problem-dependent. Figure 2 illustrates a possible state encoding in the BlockWorld game state from Figure 1. In this case, we added a special node representing the ground. Both the current state and the goal are encoded as a graph, with different edge types, and their representation is combined. Note that the nodes do not contain any label-related features.

## Actions

The problems of our focus require actions with symbolic parameters, in our case, the objects. To be as general as

possible, let’s divide the possible actions into several groups:

**Elementary actions** do not require any parameters. Examples of such actions are: *turn-left*, *accelerate* or *stop*.

**Single-parameter actions** accepts a single object. When the model selects such an action, it also needs to select a corresponding object to be its parameter. Examples of such actions are *pick(X)* or *open(X)*.

**Multi-parameter actions** require several objects as their parameters. We assume that there is a conditional dependence between the parameters (e.g., in *move(X, Y)*, the choice of  $Y$  depends on the selected  $X$ ) and hence the model has to select the objects consecutively.

**Independent-parameter actions** can have arbitrary number of parameters, independent of each other. As an example, *select(X, ...)* can be used to simultaneously select a number of objects.

Not all action may be applicable in a particular state. As an example, an *open(X)* action may be unavailable unless the object  $X$  contains a feature specifying it is closed. The availability is indicated by action’s *pre-condition* and is state-dependent.

The action space  $\mathcal{A}$  is problem-dependent and also state-dependent (the number of objects may change, pre-conditions may disable some actions). For instance, in the game of BlockWorld, there is a single two-parameter action *move(X, Y)* with a pre-condition that there is no block on top of  $X$ , and neither on  $Y$  (unless  $Y$  is the ground).

## Method

With the defined problem, several technical issues remain to be solved. First, we propose a specific instance of GNNs (Zhou et al. 2018) to process the complex state. Second, we need a way to implement the policy defined with the complex actions. We use auto-regressive policy decomposition (Vinyals et al. 2017) to tackle the multi-parameter actions. Third, several minor obstacles need to be resolved, as described below.

After we have created a differentiable model that can accept any complex state and produce a proper probability distribution over the possible actions, we can use any existing policy gradient algorithm (Li 2018) to train the model.

## State processing

Because the state is represented as a graph, the natural choice is to use a Graph Neural Network (GNN) (Zhou et al. 2018) as our model. GNNs have strong relational inductive biases (Battaglia et al. 2018) and their operations are local and invariant of node permutations. Also, the same model can be used to process states with different number of objects. There exists a number of different GNN variations, with a unifying framework made by Battaglia et al. (2018). Instead of using a particular variant, we borrow several key techniques to overcome specific obstacles.

First, let us define the input graph as follows. Let  $\mathcal{V} = \{v_i\}_{i=1..|\mathcal{V}|}$  be a set of nodes, where  $v_i$  denotes a feature vector of a node.  $\mathcal{E} = \{(e_i, s_i, r_i)\}_{i=1..|\mathcal{E}|}$  is a set of edges, where  $e_i$  is a feature vector of an edge,  $s_i$  denotes the sending node index and  $r_i$  the receiving node index of this edge. Let  $g$

be a feature vector of a special *global* node not included in  $\mathcal{V}$ . If available, the  $g$  vector is set to encode the global context, else it is zero.

The core of the algorithm is a single message-passing step defined as follows. First, the aggregated incoming messages are computed as  $m_i = \max_{r_k=i} \phi_{msg}(v_{s_k}, e_k)$ . Here,  $\phi_{msg}$  is a message embedding function, which transforms an incoming message from node  $v_{s_k}$  over an edge  $e_k$ . All messages to a node  $i$  are aggregated with an element-wise *max* function. Another common aggregation operator is *mean* (Battaglia et al. 2018); we choose *max* early in our experiments, where it worked best. Second, all node features are updated with newly computed values  $v'_i$ :

$$v'_i = v_i + \phi_{agg}(v_i, m_i, g) \quad (1)$$

The aggregated messages are processed with function  $\phi_{agg}$ , which also takes the current embedding  $v_i$  and the global node features  $g$ . In practice, we implement the  $\phi_{msg}$  and  $\phi_{agg}$  functions as single non-linear neural network layers. Finally, the addition of the original  $v_i$  vector represents a skip connection (Kipf & Welling 2016; He et al. 2016), which we found to facilitate learning in cases with a large stack of multiple message-passing steps.

After all node representations are updated, a global node  $g$  aggregates information from all other nodes through an attention mechanism:

$$g' = g + \phi_{glb}\left(g, \sum_{i=1..|\mathcal{V}|} \phi_{att}(v_i) \cdot \phi_{feat}(v_i)\right) \quad (2)$$

In here, the  $\phi_{att}$  denotes a softmax distribution over all nodes  $\mathcal{V}$ ,  $\phi_{feat}$  a node embedding function and  $\phi_{glb}$  is a final embedding function. In implementation,  $\phi_{att}$  is a single linear layer followed by softmax and  $\phi_{feat}$  and  $\phi_{glb}$  are single non-linear layers. Again, adding the original  $g$  serves as a skip connection to facilitate learning.

The steps (1) and (2) form a single message-passing step. During the computation, several steps are performed, yielding the final embeddings  $v_i, g$ . Instead of reusing the same parameters in every step, we chose to parametrize the  $\phi$  functions with an independent set of parameters for each step (see Battaglia et al. 2018). In this way, the model can compute progressively more complex representations, similar to as convolutional neural networks do (LeCun et al. 2015).

## The policy

The probability distribution over all possible actions forms the policy  $\pi$ . The action space grows exponentially with the number of actions' arguments. However, with the right policy decomposition, the complexity can be transformed into a sequential selection process. For a particular action  $a$ , let  $a^0$  denote the action identifier (e.g. *stop*, *move*, etc.) and  $a^1, a^2, \dots$  the parameters; let  $L(a)$  be the arity of action  $a$ . The policy can then be represented in an auto-regressive manner (Vinyals et al. 2017):

$$\pi(a|s) = \prod_{l=0}^{L(a)} \pi(a^l|a^{<l}, s)$$

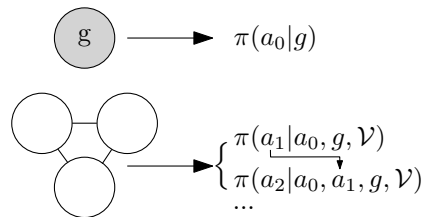


Figure 3: After several GNN passes, the final embeddings of nodes are used to decode the actions. First, the action identifier  $a_0$  (e.g., *push-left*) is selected, based on the global context  $g$ . The parameters are selected sequentially, conditioned on previous selection. The selection is input back into the network as a parameter, two message-passes are performed and next parameter is selected.

The policy is decomposed into a sequence of products, where each depends on the previously selected sub-actions. Vinyals et al. (2017) disregard the conditional dependency on the previously chosen sub-actions for implementation difficulties. However, this variant, which can be thought of a product of marginal distributions, cannot represent every possible probability distribution. Moreover, for some actions, the previously selected parameters are crucial for further selection. E.g. in *move(X, Y)*, the selection of  $Y$  only makes sense with a known  $X$ . Therefore, we propose a method to preserve the conditional dependency below.

First, let's assume that all required information about a state was encoded by the GNN in the previous step into the final node embeddings  $\mathcal{V}$  and the global context  $g$ , hence  $\pi(a|s) = \pi(a|g, \mathcal{V})$ . The process of action selection is illustrated in Figure 3. If we disregard the pre-conditions for now, the number of  $a^0$  actions is static. Hence it makes sense to select the action identifier with only the global context,  $a^0 \sim \pi(g)$ , with a single softmax head.

For the elementary actions without parameters, the decision is terminal. For parametrized actions, the parameters are dependent on the action identifier and previously selected parameters,  $a^l \sim \pi(a^0, a^1, \dots, a^{l-1}, g, \mathcal{V})$ . The actions identifiers usually have substantially different meanings, therefore, to select the first parameter  $a^1$ , we propose to use a separate head for each possible  $a^0$ . We implement this as a shared linear layer over each node's embedding  $v_i \in \mathcal{V}$  and taking softmax over all nodes (for each  $a^0$ ).

To select the parameter  $a^l, l \geq 2$ , we implement this by augmenting the existing node embeddings  $\mathcal{V}$  with one-hot encoding of previous selection  $a^{1..l-1}$ . Every node is augmented with a binary vector  $z$  of size  $l-1$ , where  $z_i$  denotes whether this node was selected at step  $i$ . To preserve the original embedding size, the augmented vector is first transformed to its original size with a single non-linear layer. Next, two message-passing steps are used to allow the information to spread globally through the global context, which creates new embeddings  $\mathcal{V}', g'$ . The parameter is selected in the same manner as with  $a^1$ , with a linear layer over all embeddings  $\mathcal{V}'$  and taking softmax (separate head for each action parameter). Note, that the new embeddings  $\mathcal{V}', g'$  are then discarded and the next parameter  $a^{l+1}$  uses the original  $\mathcal{V}, g$ .

**Pre-conditions** Some actions may be unavailable in a particular situation. The availability is resolved for the currently processed level (e.g., for  $a_0, a_1, \dots$ ), and the unavailable actions are removed from the softmax computation. In the most general case, it may happen that no selection is possible for a particular level  $l$ . In that case, we have to backtrack, disable the selection at level  $l - 1$  that led to the situation and select a new argument.

**Independent-parameter actions** These actions accept arbitrary number of independent parameters, e.g.  $select(X, \dots)$  may be used to select multiple objects at the same time. To perform such selection, we can use concurrent actions (Harmer et al. 2018). A shared function with sigmoid activation is used to compute per-node probabilities  $p(v)$ . Selection of nodes is then regarded as independent Bernoulli trials. Let  $\Upsilon$  be the set of selected nodes; the total probability for this action is then  $\pi(a_0|g) \prod_{v \in \Upsilon} p(v) \prod_{v \in \mathcal{V} \setminus \Upsilon} (1 - p(v))$ .

### Model training

Let  $\theta$  be the model parameters – a union of all  $\phi$  functions and layers used in the action selection. Each state is processed as described an a specific action  $a$  is chosen, with its probability  $\pi_\theta(a|s)$ . Also, the model outputs a value estimate of a state, dependent on the final global context,  $V_\theta(s) = V_\theta(g)$ , implemented as a single linear layer.

The policy  $\pi_\theta$  and value function  $V_\theta$  are fully differentiable and any policy-gradient based Deep RL algorithm can be used to optimize the reward. Here, we propose to use A2C algorithm, a synchronous version of A3C (Mnih et al. 2016), with a few optimizations.

Let  $Q(s, a) = \mathbb{E}_{s' \sim t(s, a)} [r(s, a, s') + \gamma V_\theta(s')]$  be a state-action value function and  $A(s, a) = Q(s, a) - V_\theta(s)$  an advantage function. Then, the policy gradient  $\nabla_\theta J$  and the value function loss  $L_V$  are:

$$\nabla_\theta J = \mathbb{E}_{s, a \sim \pi_\theta, t} \left[ A(s, a) \cdot \nabla_\theta \log \pi_\theta(a|s) \right] \quad (3)$$

$$L_V = \mathbb{E}_{s, a, s' \sim \pi_\theta, t} \left[ q(s, a, s') - V_\theta(s) \right]^2 \quad (4)$$

where the target  $q$  is:

$$q(s, a, s') = \begin{cases} r(s, a, s') & \text{if } s' \text{ is terminal} \\ r(s, a, s') + \gamma V_{\theta'}(s') & \text{else} \end{cases}$$

To prevent a target run-away problem in  $L_V$ , the  $V_{\theta'}(s')$  is estimated using a copy of parameters  $\theta'$  that are regularly updated with  $\theta' := (1 - \rho)\theta' + \rho\theta$  (Lillicrap et al. 2016), with  $\rho \in (0, 1]$ . An entropy regularization term  $L_H$  is:

$$L_H = \mathbb{E}_{s \sim \pi_\theta, t} \left[ H_{\pi_\theta}(s) \right]; H_\pi(s) = - \mathbb{E}_{a \sim \pi(s)} \left[ \log \pi(a|s) \right] \quad (5)$$

However, the precise computation of the policy entropy is intractable in our case – only single  $\pi(a|s)$  for the actually performed action  $a$  is available. Therefore, we rewrite the entropy in its gradient form and sample the expectation (Zhang et al. 2018):

$$\nabla_\theta H_{\pi_\theta}(s) = - \mathbb{E}_{a \sim \pi_\theta(s)} \left[ \log \pi_\theta(a|s) \cdot \nabla_\theta \log \pi_\theta(a|s) \right]$$

The final gradient is  $\nabla_\theta (-J + \alpha_v L_V - \alpha_h L_H)$ , with  $\alpha_v, \alpha_h$  being learning rate coefficients. We simulate a batch of parallel environments to gather a better gradient estimate. Per each step of the environment, we perform a single gradient step with AdamW (Loshchilov & Hutter 2017).

**Entropy regularization normalization** As one of our contributions, we propose a *normalization* of the entropy regularization. Standard environments where Deep RL is deployed usually have a fixed action space. Although the possible magnitude of the  $L_H$  term depends on the action space size, it is easily absorbed in the  $\alpha_h$  coefficient. In our case, the number of actions is state-dependent and therefore the maximal magnitude varies; moreover the desired property of our model is a good generalization over different problem sizes. Let  $|\mathcal{A}(s)|$  be the number of actions in a particular state  $s$ , then the maximal policy entropy is  $H_{max}(s) = \log |\mathcal{A}(s)|$ ; the proof is trivial. To stabilize the training, we propose to normalize the  $L_H$  term with the maximal possible entropy in a particular state:  $L_H = \mathbb{E}_{s \sim \pi_\theta, t} \left[ \frac{H_{\pi_\theta}(s)}{H_{max}(s)} \right]$ . In states with only a single available action,  $H_{max}(s)$  is zero and such state is excluded from the  $L_H$  computation. Preliminary results indicate that this technique is helpful to stabilize training on problems of different sizes, without tweaking  $\alpha_h$ .

## Experiments

To demonstrate the generality and performance of our method, we provide implementation and experimental results in three distinct domains. Each of the tested domain focus on a slightly different aspect – in BlockWorld, we showcase a two-parameter action and measure generalization over different variants of the problem; in Sokoban, five single-parameter actions are used, and we demonstrate facilitated curriculum learning; in SysAdmin, we demonstrate independent-parameter actions. Where applicable, we provide comparisons to the competitive methods. As a part of this paper, we release the implementation based on an open-source GNN library PyTorch Geometric (Fey & Lenssen 2019). The exact setup, model architecture and hyper-parameters are described in the Appendix.

**Time-limits** The used environments are not restricted by any time horizon, hence we use a discount factor  $\gamma = 0.99$  in all domains. However, the agent can be stuck in a situation where no action sequence leads to a goal (e.g., by misplacing a box in Sokoban). To mitigate this issue, we use a method of Pardo et al. (2018) and define an artificial time-limit for each domain, which we treat as an auxiliary property not included in the environment. That is, if the environment terminates only due to the exceeded time-limit, the next state  $s'$  is not considered terminal in the computation of target  $q$  in eq. (4).

### BlockWorld

BlockWorld is a well known domain with tractable satisficing planning and NP-hard optimal planning (Slaney & Thiébaux 2001). In RRL, its variant was studied by Džeroski et al. (2001) and more recently by Payani & Fekri (2020).

**Domain definition** The objects in the BlockWorld problem consist of a set of  $N$  blocks  $\mathcal{B} = \{b_1, b_2, \dots, b_N\}$  and a special object  $G$ , representing the ground. Let's define a relation  $x \dashv y; x \in \mathcal{B}, y \in \mathcal{B} \cup G$ , meaning that a block  $x$  is positioned on top of  $y$ . For each  $x$ , the relation is unique, as well as for each  $y$ , unless  $y = G$ . Let  $\mathcal{R}$  be a set of all relations in the problem. The action  $move(x, y)$  removes all relations  $x \dashv z; \forall z$  from  $\mathcal{R}$  and creates a new one  $x \dashv y$ . The pre-conditions for the action are  $x \neq y$ ,  $free(x)$  and  $free(y) \vee y = G$ , where  $free(x) \Leftrightarrow \nexists z : z \dashv x$ .

The goal is to use the action  $move$  to reconfigure the block positions  $\mathcal{R}_{start}$  into  $\mathcal{R}_{goal}$ . To incentivize the agent to find the optimal solution, it receives a reward  $-0.1$  for each action. After reaching the goal, the episode ends with a reward 10.

**State and actions** The state consists of the objects  $\mathcal{B}, G$ , the current set of relations  $\mathcal{R}$  and the goal  $\mathcal{R}_{goal}$  (see Figure 2 for illustration). In the graph, each relation is modeled symmetrically (both *above-of* and *below-of* are included). The different types of relations are marked by their edge parameters. The objects contain a single-bit feature, differentiating between  $\mathcal{B}$  and  $G$ . Note that the block labels are completely abstract and are not present in the state in any way.

There is a single action  $move$  with two parameters. The pre-conditions are used according to their definition. If a particular block is allowed to be the first parameter of the action  $move$ , there always exists a valid second parameter (e.g.,  $G$ ). Hence, there are no dead-ends and no need to backtrack.

**Performance experiment** We train the agent in BlockWorld environment with  $N = 5$  and randomly generated initial states and goals. We perform eight independent runs and report their mean and 95%-confidence interval in Figure 4. We define a single epoch to be 256 000 environment steps (256 parallel environments, 1000 steps each). On our reference machine (AMD Ryzen 1900X with 4 threads, 6 GB of RAM, single nVidia Titan X), a single epoch takes about 3.3 minutes; 100 epochs about 5.5 hours.

In Figure 4 we report the agent's capability to solve the environment and its optimality. After each episode, we evaluate it on 1000 random problems with  $N = 5$ , and measure the percentage of solved problems and the average ratio of number of optimal steps and performed steps for each problem. In case the agent does not solve the environment in the 100 step limit, we consider the ratio to be 0.

At about epoch 75, the agent learns to solve the problems with 100% accuracy and 83% optimality. Subsequently, the optimality increases; in epoch 200 it's 96%, and it reaches 99% in epoch 400. Hence, it can be said that the agent is able to learn near-optimal policy in this settings.

In the next experiment, we investigated whether the agent can solve a slightly more difficult environment without the pre-conditions. That is, all actions are available, however the nonsensical actions does not change the state. Our experiment confirms that the agent learns to ignore the nonsensical actions, however, the training time is almost doubled. In this case, the agent solves 100% of problems at about epoch 130 and reaches 99% optimality at about epoch 730. This experiment confirms that the pre-conditions are not necessary, but greatly help the agent's training.

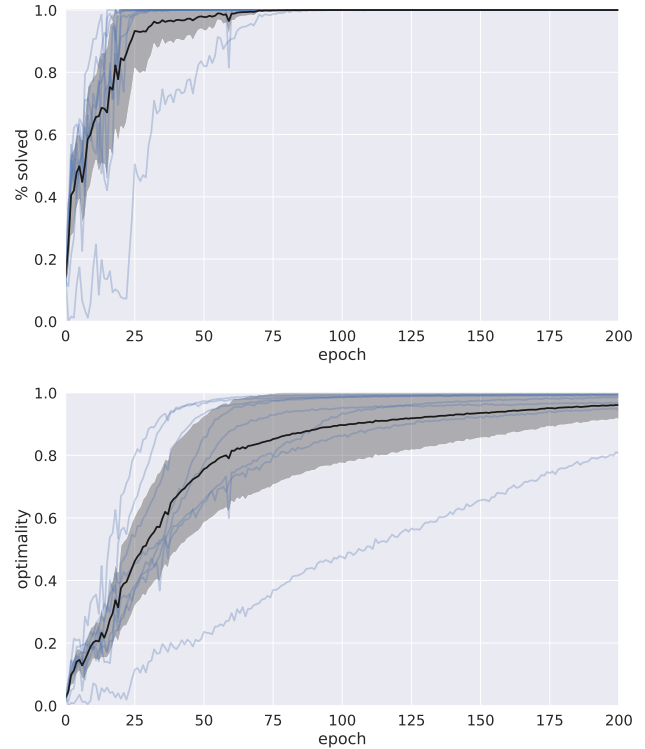


Figure 4: Training in the BlockWorld environment,  $N = 5$ . The  $x$ -axis shows epochs, where each epoch equals 256 000 environment steps. During training, the agent is evaluated on 1000 randomly generated problems (with  $N = 5$ ). The top graph shows the percentage of solved problems, the bottom shows agent's optimality (optimal / performed steps). Eight randomly initialized runs are displayed, with their mean and 95%-confidence interval.

**Generalization experiment** As the second major experiment, we focused on the generalization capabilities of the agent in environments with different number of blocks. From the eight runs with  $N = 5$ , we picked the one that performed best after 800 epochs. Next, we evaluated it in environments with different number of blocks,  $N \in \{2..20\}$ . Again, we measured the percentage of solved environments, with the 100 step limit, and also the agent's optimality (again, as the average ratio of optimal and performed steps). Given that in BlockWorld, the optimal planning is NP-hard, we report the optimality only for  $N \leq 10$ ; it becomes too expensive to compute with higher  $N$ .

The results, reported in Figure 5, show impressive generalization capabilities. The agent trained only on problems with 5 blocks solves all problems in the range  $N \leq 5$  with near-100% optimality, with an exception of  $N = 3$ . With  $N \geq 6$ , the performance gradually decreases to 78% for  $N = 20$ . The optimality decreases to with 87% for  $N = 10$ .

When we tried to train an agent directly with  $N = 10$ , the training completely failed. Yet, the agent trained with  $N = 5$  is able to solve 98% of problems with  $N = 10$ , with 87% optimality. Moreover, it gracefully generalizes up



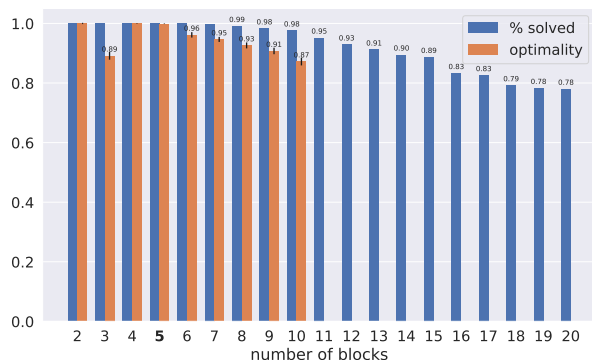


Figure 5: The agent trained only on BlockWorld with 5 blocks ( $N = 5$ ) is evaluated in problems with  $N \in \{2..20\}$ . For each  $N$ , the agent is evaluated in 1000 problems and the percentage of solved problems and its optimality is reported. The agent shows impressive generalization over the whole tested range.

to  $N \leq 20$ , possibly even more. This indicates a strong potential for curriculum learning (Bengio et al. 2009). To understand how impressive these results are, we note that the number of all possible block configurations raise very quickly with  $N$ . Exactly, it is  $\sum_{i=0}^N \binom{N}{i} \frac{(N-1)!}{(i-1)!}$  (Slaney & Thiébaux 2001); i.e., 501 for  $N = 5$ ,  $5.8 \times 10^7$  for  $N = 10$  and  $2.7 \times 10^{20}$  for  $N = 20$ . The number of actions is  $|\mathcal{A}| \leq N^2$ .

**Comparison to prior-art** Džeroski et al. (2001) investigated RRL with inductive logic programming. They focused on a more restrictive BlockWorld variant, with only three specific goals: stacking into a single tower, unstacking everything to the ground or single relation  $a \dashv b$ . For each of these goals, a specialized policy was created. However, these specific goals are trivial compared to the setting we use (any block configuration as a goal). Hence, the exact comparison is impossible without carefully reimplementing and evaluating the former method. In the published results, Džeroski et al. (2001) also showed some degree of generalization of their algorithm to the different number of blocks (3 to 10).

Recently, Payani & Fekri (2020) approached the RRL problem with differentiable inductive logic programming, in which a set of predicates is defined and their probabilities are learned by gradient descent. The advantage of the approach is that alternative high-level predicates can be included to facilitate the learning. The work also focuses on the BlockWorld problem, with an input represented as an image. However, it is unclear if their approach scales and generalizes, as the authors only train and evaluate their algorithm with 4 and 5 blocks.

### Sokoban

Results to be published.

### SysAdmin

Results to be published.

## Conclusion

We presented a novel generic framework, based on deep reinforcement learning and graph neural networks, for solving problems in relational domains. The method operates with a symbolic representation of objects and their relations and actions manipulating them. We described a generic way to implement multi-parameter actions, where the arguments are mutually dependent, and concurrent actions. Our experiments indicate that one of the main advantages of our approach is a powerful generalization to different problem variants, enabled by the relational inductive bias. For example, in BlockWorld, the agent trained only on problems with 5 blocks works remarkably well on problems with different amount of blocks, from 2 to 20. With 10 blocks, it solves 98% of problems with 87% optimality, although the training directly with 10 blocks failed. With 20 blocks, it solves 78% of problems.

We are yet to demonstrate our method in two more domains: Sokoban and SysAdmin. In Sokoban, our preliminary experiments show that the method greatly outperforms imagination augmented agents by Racanière et al. (2017) and is competitive with Deep RL planning agents of Guez et al. (2019). In SysAdmin, we will showcase our framework’s overreach to the planning domain and compare it to the state-of-the-art PROST planner (Keller & Eyerich 2012).

## Acknowledgments

We thank Dan Fišer for a discussion about planners. This research was supported by the European Office of Aerospace Research and Development (grant no. FA9550-18-1-7008) and by The Czech Science Foundation (grants no. 18-21409S and 18-27483Y). The access to the computational infrastructure of the OP VVV funded project CZ.02.1.01/0.0/0.0/16\_019/0000765 “Research Center for Informatics” is gratefully acknowledged. Some GPUs used in this research were donated by the NVIDIA Corporation.

## References

- Adjodah, D., Klinger, T., and Joseph, J. Symbolic relation networks for reinforcement learning. *Relational Representation Learning Workshop*, 2018.
- Bajpai, A. N., Garg, S., et al. Transfer of deep reactive policies for mdp planning. In *Advances in Neural Information Processing Systems*, pp. 10965–10975, 2018.
- Battaglia, P. W., Hamrick, J. B., Bapst, V., Sanchez-Gonzalez, A., Zambaldi, V., Malinowski, M., Tacchetti, A., Raposo, D., Santoro, A., Faulkner, R., et al. Relational inductive biases, deep learning, and graph networks. *arXiv preprint arXiv:1806.01261*, 2018.
- Bengio, Y., Louradour, J., Collobert, R., and Weston, J. Curriculum learning. In *Proceedings of the 26th annual international conference on machine learning*, pp. 41–48, 2009.
- Džeroski, S., De Raedt, L., and Driessens, K. Relational reinforcement learning. *Machine learning*, 43(1-2):7–52, 2001.
- Fey, M. and Lenssen, J. E. Fast graph representation learning with PyTorch Geometric. In *ICLR Workshop on Representation Learning on Graphs and Manifolds*, 2019.
- Garnelo, M., Arulkumaran, K., and Shanahan, M. Towards deep symbolic reinforcement learning. *arXiv preprint arXiv:1609.05518*, 2016.

- Guestrin, C., Koller, D., and Parr, R. Max-norm projections for factored mdps. In *IJCAI*, volume 1, pp. 673–682, 2001.
- Guez, A., Mirza, M., Gregor, K., Kabra, R., Racanière, S., Weber, T., Raposo, D., Santoro, A., Orseau, L., Eccles, T., et al. An investigation of model-free planning. *arXiv preprint arXiv:1901.03559*, 2019.
- Hamrick, J. B., Allen, K. R., Bapst, V., Zhu, T., McKee, K. R., Tenenbaum, J., and Battaglia, P. W. Relational inductive bias for physical construction in humans and machines. In Kalish, C., Rau, M. A., Zhu, X. J., and Rogers, T. T. (eds.), *Proceedings of the 40th Annual Meeting of the Cognitive Science Society, CogSci 2018, Madison, WI, USA, July 25-28, 2018*, 2018.
- Harmer, J., Gisslén, L., del Val, J., Holst, H., Bergdahl, J., Olsson, T., Sjö, K., and Nordin, M. Imitation learning with concurrent actions in 3d games. In *2018 IEEE Conference on Computational Intelligence and Games (CIG)*, pp. 1–8. IEEE, 2018.
- He, K., Zhang, X., Ren, S., and Sun, J. Deep residual learning for image recognition. In *Proceedings of the IEEE conference on computer vision and pattern recognition*, pp. 770–778, 2016.
- Helmert, M. The fast downward planning system. *Journal of Artificial Intelligence Research*, 26:191–246, 2006.
- Helmert, M. and Domshlak, C. Lm-cut: Optimal planning with the landmark-cut heuristic. *Seventh international planning competition (IPC 2011), deterministic part*, pp. 103–105, 2011.
- Jaderberg, M., Czarnecki, W. M., Dunning, I., Marris, L., Lever, G., Castaneda, A. G., Beattie, C., Rabinowitz, N. C., Morcos, A. S., Ruderman, A., et al. Human-level performance in 3d multiplayer games with population-based reinforcement learning. *Science*, 364(6443):859–865, 2019.
- Keller, T. and Eyerich, P. PROST: Probabilistic planning based on UCT. In *Proceedings of the Twenty-Second International Conference on Automated Planning and Scheduling (ICAPS 2012)*, pp. 119–127. AAAI Press, 2012.
- Kipf, T. N. and Welling, M. Semi-supervised classification with graph convolutional networks. *arXiv preprint arXiv:1609.02907*, 2016.
- LeCun, Y., Bengio, Y., and Hinton, G. Deep learning. *Nature*, 521(7553):436–444, 2015.
- Leibo, J. Z., d’Autume, C. d. M., Zoran, D., Amos, D., Beattie, C., Anderson, K., Castañeda, A. G., Sanchez, M., Green, S., Gruslys, A., et al. Psychlab: a psychology laboratory for deep reinforcement learning agents. *arXiv preprint arXiv:1801.08116*, 2018.
- Li, R., Jabri, A., Darrell, T., and Agrawal, P. Towards practical multi-object manipulation using relational reinforcement learning. *arXiv preprint arXiv:1912.11032*, 2019.
- Li, Y. Deep reinforcement learning. *arXiv preprint arXiv:1810.06339*, 2018.
- Lillicrap, T. P., Hunt, J. J., Pritzel, A., Heess, N., Erez, T., Tassa, Y., Silver, D., and Wierstra, D. Continuous control with deep reinforcement learning. In *International Conference on Learning Representations*, 2016.
- Loshchilov, I. and Hutter, F. Decoupled weight decay regularization. In *International Conference on Learning Representations*, 2017.
- Maas, A. L., Hannun, A. Y., and Ng, A. Y. Rectifier nonlinearities improve neural network acoustic models. In *International Conference on Learning Representations*, 2013.
- Mnih, V., Kavukcuoglu, K., Silver, D., Rusu, A. A., Veness, J., Bellemare, M. G., Graves, A., Riedmiller, M., Fidjeland, A. K., Ostrovski, G., et al. Human-level control through deep reinforcement learning. *Nature*, 518(7540):529–533, 2015.
- Mnih, V., Badia, A. P., Mirza, M., Graves, A., Lillicrap, T., Harley, T., Silver, D., and Kavukcuoglu, K. Asynchronous methods for deep reinforcement learning. In *International Conference on Machine Learning*, 2016.
- Pardo, F., Tavakoli, A., Levdi, V., and Kormushev, P. Time limits in reinforcement learning. In *International Conference on Machine Learning*, pp. 4045–4054, 2018.
- Payani, A. and Fekri, F. Incorporating relational background knowledge into reinforcement learning via differentiable inductive logic programming. *arXiv preprint arXiv:2003.10386*, 2020.
- Pevný, T. and Somol, P. Discriminative models for multi-instance problems with tree structure. In *Proceedings of the 2016 ACM Workshop on Artificial Intelligence and Security*, pp. 83–91. ACM, 2016.
- Racanière, S., Weber, T., Reichert, D., Buesing, L., Guez, A., Rezende, D. J., Badia, A. P., Vinyals, O., Heess, N., Li, Y., et al. Imagination-augmented agents for deep reinforcement learning. In *Advances in neural information processing systems*, pp. 5690–5701, 2017.
- Sanner, S. Relational dynamic influence diagram language (rddl): Language description. *Unpublished manuscript. Australian National University*, 32:27, 2010.
- Santoro, A., Raposo, D., Barrett, D. G., Malinowski, M., Pascanu, R., Battaglia, P., and Lillicrap, T. A simple neural network module for relational reasoning. In *Advances in neural information processing systems*, pp. 4967–4976, 2017.
- Slaney, J. and Thiébaux, S. Blocks world revisited. *Artificial Intelligence*, 125(1-2):119–153, 2001.
- Vinyals, O., Ewalds, T., Bartunov, S., Georgiev, P., Vezhnevets, A. S., Yeo, M., Makhzani, A., Küttler, H., Agapiou, J., Schrittwieser, J., et al. Starcraft ii: A new challenge for reinforcement learning. *arXiv preprint arXiv:1708.04782*, 2017.
- Zaheer, M., Kottur, S., Ravanbakhsh, S., Póczos, B., Salakhutdinov, R. R., and Smola, A. J. Deep sets. In *Advances in neural information processing systems*, pp. 3391–3401, 2017.
- Zambaldi, V., Raposo, D., Santoro, A., Bapst, V., Li, Y., Babuschkin, I., Tuyls, K., Reichert, D., Lillicrap, T., Lockhart, E., et al. Deep reinforcement learning with relational inductive biases. In *International Conference on Learning Representations*, 2019.
- Zelinka, M., Yuan, X., Cote, M.-A., Laroche, R., and Trischler, A. Building dynamic knowledge graphs from text-based games. *arXiv preprint arXiv:1910.09532*, 2019.
- Zhang, Y., Vuong, Q. H., Song, K., Gong, X.-Y., and Ross, K. W. Efficient entropy for policy gradient with multidimensional action space. *arXiv preprint arXiv:1806.00589*, 2018.
- Zhou, J., Cui, G., Zhang, Z., Yang, C., Liu, Z., and Sun, M. Graph neural networks: A review of methods and applications. *arXiv preprint arXiv:1812.08434*, 2018.



## Appendix

### Model architecture & hyper-parameters

For all non-linear layers, we use LeakyReLU activation function (Maas et al. 2013), unless specified otherwise. Before processing the state in the GNN, features of each object are embedded into a fixed-length vector of size  $emb\_size$ , with a shared single non-linear layer. The same parameter  $emb\_size$  then defines the dimension of all subsequent intermediary embeddings of nodes and the global context. Edge types are one-hot-encoded and used directly. A  $mp\_steps$  message-passing steps (eqs. 1, 2) are performed to get the final embeddings  $\mathcal{V}, g$ . AdamW optimizer (Loshchilov & Hutter 2017) with a weight decay of  $1 \times 10^{-4}$  is used. Gradients exceeding  $grad\_max\_norm$  are normalized to this norm. Learning rate and entropy regularization coefficient  $\alpha_h$  are annealed, from their respective starting values  $LR_{start}, \alpha_{hstart}$ , until their minimum  $LR_{end}, \alpha_{hend}$ . Learning rate annealing schedule is step-based, with a factor 0.5 used every  $20 \times epoch$  steps. Coefficient  $\alpha_h$  is annealed based on  $\frac{1}{t}$  schedule, where  $t$  is increased per each  $epoch$  steps. For each environment, we define a  $q\_range$  interval, that is used to clip the target  $q$  in eq. 4. A batch of  $p\_envs$  parallel environments is simulated on several CPUs. The model itself is processed and optimized using a single GPU. Other hyper-parameters are available in Table A.1.

### Other details

We measured the number of optimal steps in BlockWorld using Fast Downward planner (Helmert 2006) with A\* algorithm and LM-cut heuristic (Helmert & Domshlak 2011).

| parameter  | BlockWorld         | Sokoban | SysAdmin |
|--|--------------------|---------|----------|
| $p\_envs$ , batch size                           | 256                | -       | -        |
| $\rho$ , target-network update coefficient       | 0.005              |         |          |
| $\gamma$ , discount factor                       | 0.99               |         |          |
| $epoch$ , number of steps per epoch              | 1000               |         |          |
| episode step-limit                               | 100                |         |          |
| $mp\_steps$ number of GNN message-passes         | 3                  |         |          |
| $emb\_size$ , embedding size                     | 32                 |         |          |
| $LR_{start}$ , initial learning rate             | $3 \times 10^{-4}$ |         |          |
| $LR_{end}$ , final learning rate                 | $1 \times 10^{-5}$ |         |          |
| $grad\_max\_norm$ , maximal gradient             | 3.0                |         |          |
| $q\_range$ , range of target $q$ (eq. 4)         | $[-15, 15]$        |         |          |
| $\alpha_v$ , coefficient of $L_V$                | 0.1                |         |          |
| $\alpha_{hstart}$ , initial coefficient of $L_H$ | $1 \times 10^{-4}$ |         |          |
| $\alpha_{hend}$ , final coefficient of $L_H$     | $5 \times 10^{-5}$ |         |          |

Table A.1: Hyper-parameters used in the experiments